Int. J. Cancer: **101,** 360–370 (2002)

Publication of the International Union Against Cancer

LABELED EGFR-TK IRREVERSIBLE INHIBITOR (ML03): *IN VITRO* AND *IN VIVO* PROPERTIES, POTENTIAL AS PET BIOMARKER FOR CANCER AND FEASIBILITY AS ANTICANCER DRUG

Giuseppina ORTU[1,2], Iris BEN-DAVID[1], Yulia ROZEN[1], Nanette M.T. FREEDMAN[3], Roland CHISIN[3], Alexander LEVITZKI[2] and Eyal MISHANI[1]*

[1]*Hebrew University, Hadassah University Hospital Campus, Department of Medical Biophysics and Nuclear Medicine, Jerusalem, Israel*
[2]*Hebrew University, Givat Ram Campus, Department of Biological Chemistry, Institute of Life Sciences, Jerusalem, Israel*
[3]*Hadassah University Hospital Campus, Department of Medical Biophysics and Nuclear Medicine, Jerusalem, Israel*

Radiosynthesis of ML03 (*N*-{4-[(4,5-dichloro-2-fluorophenyl)-amino]quinazolin-6-yl}acrylamide), an irreversible EGFr-TK inhibitor, was developed. Its *in vitro* and *in vivo* properties, its potential as PET biomarker in cancer and the feasibility of this type of compounds to be used as anticancer drug agents were evaluated. The compound was labeled with carbon-11 at the acryloyl amide group, via automated method with high yield, chemical and radiochemical purities. ELISA carried out with A431 lysate showed high potency of ML03 with an apparent IC_{50} of 0.037 nM. The irreversible binding nature of ML03 was studied and 97.5% EGFr-TK autophosphorylation inhibition was observed in intact A431 cells 8 hr post incubation with the inhibitor. Specific binding (67%) of [^{11}C]ML03 was obtained in cells. An A431 tumor-bearing rat model was developed and the validity of the model was tested. In biodistribution studies carried out with tumor-bearing rats, moderate uptake was observed in tumor and high uptake in liver, kidney and intestine. In metabolic studies, fast degradation of [^{11}C]ML03 was observed in liver and blood indicating a short half-life of the compound in the body. PET scan with tumor-bearing rats confirmed the results obtained in the *ex vivo* biodistribution studies. Although *in vitro* experiments may indicate efficacy of ML03, non-specific binding, ligand delivery and degradation *in vivo* make ML03 ineffective as PET bioprobe. Derivatives of ML03 with lower metabolic clearance rate and higher bioavailability should be synthesized and their potential as anticancer drugs and PET bioprobes evaluated.

Key words: *carbon-11; cancer; biodistribution; PET; EGFr*

Growth factors mediate their pleiotropic actions by binding to and activating receptor tyrosine kinases. Epidermal growth factor receptor (EGFr, erb-B1) belongs to a family of proteins involved in the proliferation of normal and malignant cells.[1,2] The binding of activating ligands such as EGF, TGF α, AR, BTC or HB-EGF to the EGFr results in activation of the cytosolic kinase domain. Overexpression of EGFr is the hallmark of many human tumors such as breast cancer, glioma, laryngeal cancer, squamous cell carcinoma of the head and neck and prostate cancer.[3] Since the late 1980s continuous effort has been invested in the development of EGFr tyrosine kinase inhibitors as anti-neoplastic drugs.[4,5–11] Radioactively labeled small molecules with high affinity and selectivity for the tyrosine kinase domain of EGFr might offer a specific and sensitive tool to be used in positron emission tomography (PET) for diagnosis of tumors overexpressing EGFr. PET provides 3D and quantitative maps of the distribution of radioactive tracers within the human body and hence permits the measurement of physiological, biochemical and pharmacological function at the molecular level, both in healthy and pathological states. PET is based on the use of short half-life positron-emitting isotopes, such as ^{11}C ($t_{1/2}$ 20.39 min.), ^{18}F ($t_{1/2}$ 109.8 min.), ^{15}O ($t_{1/2}$ 2.037 min.) and ^{13}N ($t_{1/2}$ 9.965 min.). After injection of a suitable biomarker, the PET scan provides a mapping of the biomarker distribution and hence of a specific receptor, transporter or enzyme in the human body. Biomarkers with high selectivity for a specific receptor or enzyme might accumulate in those organs and tissues where the targeted protein is overexpressed. In the case of EGFr, its overexpression in human tumors could be non-invasively detected by labeling tyrosine kinase inhibitors with positron-emitting isotopes. The PET application of these potential biomarkers represents a new strategy for the diagnosis of EGFr-expressing tumors.[12–14] Moreover, the increasing demand to incorporate diagnostics into clinical studies of EGFr-targeted therapies suggests a potential future use of EGFrTK labeled inhibitors. These labeled inhibitors could help select patients for clinical trials. Cancer patients could undergo a non-invasive diagnostic PET study with labeled EGFrTK inhibitor, and if their tumor is found to overexpress EGFrTK, they could then be selected for a clinical trial that utilizes anti-EGFr therapy.

In our previous work,[15] we synthesized, labeled and evaluated 4-(fluoroanilino)quinazoline derivatives as EGFrTK PET biomarkers. These molecules bind reversibly to the ATP binding site of the receptor and inhibit the autophosphorylation of the EGFrTK. Competition with intracellular ATP results in their fast dissociation from the EGFr kinase site, however, making these compounds ineffective as PET reporter probes. We therefore concluded that irreversible EGFr tyrosine kinase inhibitors labeled with carbon-11 might be more effective as PET markers for tumors overexpressing EGFr.

A group of compounds (6-acrylamido-4-anilinoquinazolines) that bind irreversibly to the EGFr have been described recently.[16–20] The ligand binds covalently to the cys-773, which is proximal to the ATP binding site.[20] The irreversible binding blocks EGFr function, leading to growth inhibition and apoptosis.[16]

On the basis of these findings, we present the biological evaluation of a novel EGFr-TK irreversible inhibitor, *N*-{4-[(4,5-dichloro-2-fluorophenyl)amino] quinazolin-6-yl}acrylamide (ML03, Fig. 1). This molecule was successfully labeled with carbon-11 in the acryloyl group and evaluated *in vitro* and *in vivo* as a PET tracer for EGFrTK-overexpressing tumors.

Abbreviations: AR, amphireguline; BTC, betacelluline; EGF, epidermal growth factor, EGFr, epidermal growth factor receptor; HB-EGF, heparin-binding EGF-like growth factor; PET, positron emission tomography; TK, tyrosine kinase; TGFα, transforming growth factor α.

Grant sponsor: USA-Israel Bi-National Science Foundation; grant number: BSF 98000082.

*Correspondence to: Hadassah University Hospital, Department of Nuclear Medicine, IL-91120, Jerusalem, Israel. Fax: +972-2-6421203.
E-mail: mishani@md2.huji.ac.il

Received 2 May 2002; Revised 13 June 2002; Accepted 21 June 2002

DOI 10.1002/ijc.10619

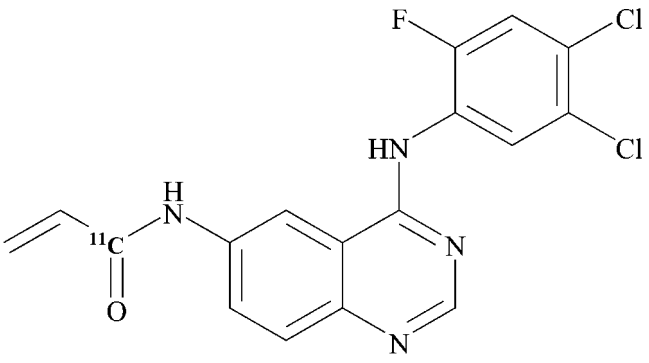

FIGURE 1 – *N*-{4-[(4,5-dichloro-2-fluorophenyl)amino]quinazolin-6-yl}acrylamide (ML03).

MATERIAL AND METHODS

Preparation of unlabeled and labeled ML03 21

Unlabeled ML03 was prepared as described by Mishani *et al*.[21] Carbon-11 labeled ML03 was prepared by an automated synthesis. One Curie of trapped [C-11]CO_2, was transferred to a first reactor. After addition of phthaloyl dichloride and di-*tret*-butylpyridine, the reactor was heated to 90°C and [C-11]acryloyl chloride was distilled with a flow of argon (first at 25 mL/min for 2 min and then 30 mL/min) to a second reactor. Reactor 2 contained 3.5 mg of 6-amino-4-(3,4-dichloro-6-fluoroanilino)-quinazoline in 0.5 mL of dry THF at −5°C. After 7-min distillation, the temperature in reactor 2 was increased to 30°C, 0.7 mL of HPLC solvent was added and the solution was injected into the built in HPLC (mobile phase, 46 % acetonitrile, 54% acetate buffer 0.1 M pH 3.8, flow 13 ml/min). The product (Rt, 22 min) was collected into the solid phase extraction vial containing 70 mL of water and 2.5 mL of NaOH (1 M). The solution was passed through a C-18 cartridge (activated with 10 mL EtOH and 10 mL of sterile water). The cartridge was then washed with 10 mL of sterile water. The product was eluted with 0.7 mL of EtOH, followed by 4.3 mL of saline, collected into the product vial containing 50 μL of 0.1 M HCl, and transferred through a sterile Millipore™ 0.22 μm filter to a 20-mL sterile vial placed in a lead container. The chemical and radiochemical purities were analyzed by reverse phase HPLC C-18 analytical column.

BIOLOGICAL EVALUATION OF ML03

Autophosphorylation inhibition in A431 cell lysate

Measurement of the apparent IC_{50} for ML03 was carried out as described by Bonasera *et al*.[15] Briefly, A431 cell lysate was used as the EGFr source. A 96-well ELISA plate was coated with anti-EGFr antibody and the A431 lysate added. ML03 was incubated with the lysate in several concentrations. ATP was then added to the wells (containing lysate plus inhibitor), to phosphorylate the unbound EGFrTK. The reaction was stopped by adding EDTA. Finally, anti-phosphotyrosine from rabbit and then anti-rabbit peroxidase conjugated antibody were added; a colorimetric reaction initiated by ABTS-H_2O_2 allowed the quantification of the phosphorylated EGFrTK fraction.

Autophosphorylation inhibition experiments in whole A431 cells

Cells (10^5–10^6) were seeded in 6-well plates (35 mm diameter, Nalge Nunc) and grown to 60–80% confluency (~after 24 hr from the seeding) in DMEM (high glucose) with 10% FCS, penstrep (penicillin 10^5 U/L, streptomycin 100 mg/L) (Biological Industries, Kibbutz Beit Haemek, Israel) at 37°C, 5% CO_2. To decrease the basic level of autophosphorylation, A431 cells were exposed to serum-free medium for 18 hr and afterward treated with varying amounts of inhibitor at several time points.

Two sets of experiments were carried out. In the first one, cells, after 18 hr of starvation, were incubated for 2 hr with different amounts of ML03 at 37°C, then the medium was washed away and FCS/ML03-free medium was added. Cells were then kept for 2 and 8 hr at 37°C until the EGFr was stimulated by EGF. In the set kept for 8 hr, the medium was replaced 3 times with FCS/ML03-free medium, once every 2 hr.

In the second set of experiments, starved cells were incubated for ~30 min at room temperature and then incubated with ML03 for different time ranges (from 1–60 min). One group was immediately stimulated with EGF (20 ng/ml, 5 min), whereas 2 other sets of cells were returned to 37°C, after replacing the medium with FCS/ML03-free medium. One group of cells (at 37°C) was stimulated with EGF after 2 hr whereas the remaining group was stimulated only after 8 hr. In this latter experiment, the medium was not replaced during the 8 hr of incubation with FCS/ML03-free medium.

The inhibitor solution was always freshly prepared and the final concentration of the vehicle was 0.05% DMSO and 0.2% EtOH. Cells were always activated with EGF and then washed with PBS. Whole-cell lysates were made by scraping the cells into the well with 0.4 mL of Laemmli buffer (10% glycerol, 3% sodium dodecyl sulfate, 5% β-mercaptoethanol, 50 mM Tris pH 6.8) containing 0.001% bromophenol blue and then boiled for 5 min. Each sample was kept at −20°C until the protein determination assay.

The amount of protein in each lysate was determined by a filter paper assay described by Bonasera *et al*.[15] The same amount of protein for each sample was then loaded onto an acrylamide gel for a Western blot assay. Blots were incubated with anti-phosphotyrosine, followed by incubation with horseradish peroxidase-conjugated secondary antibody. EGFr-TK bands were visualized using chemiluminescent detection.

In vitro *studies with [^{11}C]ML03: determination of specific binding in intact A431 cells*

Samples of 1.6×10^5 A431 cells (~3.2 pmol of EGFr-TK) were harvested into tubes with 2 mL of DMEM + 10% FCS and preincubated for 40 min at room temperature under shaking conditions. One set of tubes was incubated with unlabeled ML03 (1 nmol) for determination of the non-specific binding, whereas another set of cells was incubated only with the inhibitor vehicle (0.2% DMSO). [^{11}C]ML03 (from 5–80 pmol, in EtOH solution, 0.2% final concentration) was then added to both tube sets for 20 min at room temperature. For each quantity of [^{11}C]ML03 added, 2 tubes did not contain A431 cells but only medium (+ unlabeled ML03 for the non-specific binding set) and these samples were used to check the non-specific retention of the compound on the filters. After the incubation, cells were harvested with a cell harvester (YEDA Scientific Instruments, Rehovot, Israel) and the tubes washed twice with PBS. The GF/C filters used for the harvesting were pre-soaked in 0.3% PEI (polyethylenimine) for at least 1 day (at 4°C). Cells were then counted in a γ-counter (1480 Wizard™ 3″). Specific binding of [^{11}C]ML03 was calculated by subtracting the radioactivity of samples preincubated with unlabeled material from radioactivity of cells not preincubated with unlabeled compound. Both groups of values were corrected for filter [^{11}C]ML03 retention by subtracting the counts of the samples without A431 cells.

In vivo *studies with [^{11}C]ML03: biodistribution in tumor-bearing rats*

All experiments on living animals were carried out under the guidelines and with the approval of the Research Animal Ethics Committee of The Hebrew University of Jerusalem. A nude rat tumor implant model was developed. WAG *rnu/rnu* male rats (300–400 g) were injected s.c. in the left or right posterior leg, or in the neck with A431 (10^7 in 200 μL sterile PBS). Tumor growth was quite variable and tumor mass in the biodistribution experiments ranged between 3–9 g.

Tumor-bearing rats were anesthetized either with pentothal (85 mg/Kg, i.p.) or ether (although it is known that pentothal might enhance the P450 cytochrome activity in the liver, we found no difference in the biodistribution of the ligand or in the metabolic studies when animals are anesthetized with ether or pentothal) and injected i.v. in the tail with [^{11}C]ML03 (100–200 μCi, 0.44–10.53 μg/mL, in ~300 μL of SF, ~14% EtOH). Animals were sacrificed at specific time points by means of CO_2 asphyxiation. Blood and certain organs and tissues were collected or excised, counted in a γ-counter and weighed.

Validation of the tumor-bearing animal model

To evaluate the correlation between the tumor mass and the amount of EGFr per g of tumor, tumors were collected from rats and the EGFr extracted.[11,16]

EGFr extraction. Intact tumors of different mass were carefully excised from tumor-bearing rats (n = 9) and kept at −70°C until the extraction. Tumors were never thawed, to avoid the loss of the liquid component where it was present. Before the extraction, tumors were reduced to small pieces with mortar and pestle on ice and with liquid nitrogen inside the mortar. An aliquot of 1 g was weighed and homogenized on ice with polytron in 5 mL of freshly prepared lysis buffer (150 mM NaCl, 50 mM HEPES, 10% glycerol, aprotinin 1 μg/mL, leupeptin 10 μg/mL, AEBSF 1 mM, 1% sodium orthovanadate, benzaodimine ~0.3 mg/ml, soy bean trypsin inhibitor 10 μg/mL). After homogenization, 1% Triton X-100 (final concentration) was added and the samples were kept for 30 min at 4°C and rotated end over end. A subsequent centrifugation (20,000*g* × 30 min at 4°C in an Eppendorf centrifuge) allowed the separation of pellet and supernatant. The supernatant (containing EGFr) was diluted 1:1 with Laemmli buffer and boiled for 10–20 min at 100°C. Protein amounts of the boiled samples were measured as described above and then equal amounts of protein were loaded onto a gel (10% acrylamide) for a Western blot assay. In this assay (described previously) the total EGFr was determined by incubation of the blot with antibody anti-EGFr. To validate our extraction procedure, 10,[7] 2×10^7 and 3×10^7 A431 cells were extracted and diluted using exactly the same procedure described for tumors and loaded onto gel for EGFr determination.

Extraction and stability of [^{11}C]ML03 in blood and plasma

To determine the stability of our compound and its half-life in blood and plasma, [^{11}C]ML03 (~100 μL, range of mass 0.32–1.87 μg/mL, vehicle ETOH <1.5% final concentration) was incubated at 37°C with 1 mL of human blood or plasma (in glass vials), under shaking conditions. At different time points (10, 20, 30, 40, 50 and 60 min), 5 mL of ether was added to blood/plasma and the vials were counted in a γ-counter. One sample of blood and 1 of plasma were treated immediately with ether without incubation at 37°C (Time 0). The ether phase was then removed and the post-extraction fraction (erythrocytes and non-extractable ML03) was counted as well in a γ-counter. For some time points (0, 20, 40, 60 min for blood and 20, 40 and 60 min for plasma) the ether phase was loaded into $MgSO_4$ (2 g), filtered (Whatman, Puradisc 0.45 μm, polypropylene) and the volume reduced to ~100 μL under nitrogen. The small volume was then loaded onto a TLC plates (reverse phase C-18, 5 × 20 cm, 250 μm layer thickness, LKC-18F, Whatman) and run with MeOH:0.1 N NaCl = 4:1 as mobile phase. A small amount of radioactive material (10 μL of a [^{11}C]ML03 solution diluted 1:100) was spotted near the sample in each TLC as standard. After the run, TLCs were exposed for 1 hr to phosphor imager plates (Fuji), scanned with BASreader 3.1 version and analyzed with TINA 2.10 g software.

Metabolite analysis in control animals

Anesthetized control animals (male rats, 200–300 g, *rnu*/+) were injected i.v. with [^{11}C]ML03 (concentration 0.39–2.8 μg/mL, ~300 μL). At several time points (15, 30 and 60 min), 0.75 mL of blood was withdrawn from each animal with heparinized syringe from the heart and mixed immediately with 3.750 mL of ether for the extraction of radioactivity. The extraction was carried out as described above (see blood and plasma extraction). The ether phase was spotted onto TLC and the TLC exposed to phosphor imager plates after the run. As described above [^{11}C]ML03 was spotted onto the TLC as standard and run alongside the samples. Pre-extraction blood samples and extracted blood residues were counted in a γ-counter for determination of the extractable radioactivity fraction.

Metabolic studies were carried out in liver homogenates as well, using the same general procedure as for the blood samples. Control rats were injected with [^{11}C]ML03 and were sacrificed at 15 and 30 min. Blood (1 mL) was collected and ~2 g of liver were minced and homogenized with 4 mL of physiological solution in a tissue grinder (Fenbroek). Blood and homogenized liver samples were extracted as described previously, spotted onto TLC and the radioactivity was detected with phosphor imaging plates.

PET studies

PET scans were carried out on a Positron Corporation HZL/R scanner (intrinsic spatial resolution: in-plane 5.8 mm, axial 6.3 mm). The rats were anesthetized with pentothal (85 mg/Kg) and placed supine on a flat polystyrene foam support with feet taped to the support to minimize likelihood of movement. Transmission scans (duration 8 min) were obtained using a Ge-68 rotating rod. About 100–200 μCi [^{11}C]ML03 was then injected into a tail vein and scanning was started immediately. Dynamic emission scans were obtained starting at the time of injection and continuing for 60 min (10 * 30 sec, 5 * 1 min and 10 * 5 min). PET data were normalized for variations in detector sensitivity and corrected for wobble, randoms, scatter and deadtime. Attenuation correction was applied using the measured transmission scan data. PET images were reconstructed by filtered back-projection using a Butterworth filter (cut-off 0.2 cycles/mm, order 10). For comparison, a PET study with [^{18}F]FDG was also carried out on 1 rat.

Images of the attenuation and emission scans were superimposed using MPITool software (Multi Purpose Imaging Tool, Max Planck Institute, Köln, Germany). Partial biodistribution was obtained after the PET scan when the rat was injected with [^{11}C]ML03.

RESULTS

In vitro *results*

ML03 ability to inhibit the autophosphorylation of EGFr-TK was screened by ELISA. The dose–response curve shown in Figure 2 was obtained with 3 sets of values in which concentration of ML03 ranged from 6.1×10^{-8} nM to 15 nM and another set of values obtained with concentration between 1.6×10^{-9} nM and 10 nM. The curve ($r^2 = 0.84$) resulting from the combination of all values gives an apparent IC_{50} of 0.037 nM with a confidence interval ranging between 0.010 nM and 0.134 nM, indicating the high potency of ML03. According to the methodology of our assay, the ATP cannot displace ML03 that is added to the A431 lysate before ATP. The apparent IC_{50} value is a titration of the receptors still available for further ATP binding after ML03 binding. Therefore, a longer incubation time with ML03 would result in a smaller IC_{50} value.

The irreversible effect of ML03 on the EGFr-TK autophosphorylation was tested with intact A431 cells (Fig. 3). When 10^6 A431 cells (~2.0 pmol of EGFr) (for B_{max} values see Bonasera *et al.*[15]) were used (Fig. 3*a*), 100% inhibition was obtained 2 hr post-incubation with 200 pmol of ML03 (50 nM), whereas 8 hr post-incubation gave ~98% inhibition with the same amount of inhibitor. When 2×10^5 (~0.4 pmol of EGFr) A431 cells were used (Fig. 3*b*), 100% inhibition at 2 hr post-ML03 incubation was observed with 50 pmol (10 nM) of inhibitor, whereas 8 hr post ML03 incubation the inhibition was ~80%.

The inhibition rate was studied using 150 pmol of ML03, constant quantity of cells (~1,2 pmol EGFr) and different incubation time points. The results are shown in Figure 3 where the

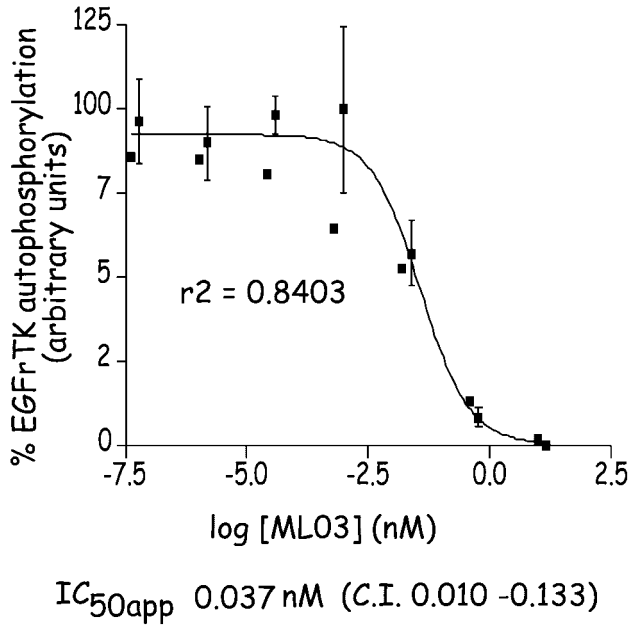

FIGURE 2 – Effect of ML03 on the EGFrTK autophosphorylation in A431 lysate (ELISA assay). The function is a sigmoidal dose response curve with variable slope. (n = 4, in parenthesis the interval of confidence of the apparent IC_{50}).

quantification of the Western blots is represented in the plots. The EGFr-TK autophosphorylation level was measured immediately after the incubation with ML03 (Fig. 3*c*), 2 hr post-incubation (Fig. 3*d*) and 8 hr post-incubation (Fig. 3*e*). In the latter case, the medium was not changed during the 8 hr, unlike in the previous experiment (Fig. 3*a*,*b*). The plots show that the EGFr-TK autophosphorylation level decreases rapidly during the first 10 min of incubation with ML03. After 60 min, 82.5% of the receptor is inhibited and this value increases when the autophosphorylation is measured 2 hr and 8 hr post-incubation, reaching 95% and 97.5% inhibition, respectively.

In vitro *studies with [^{11}C]ML03*

The specific binding of ML03 was tested by a radioactive binding assay incubating [^{11}C]ML03 with A431 cells (1.6×10^5 cells). Figure 4 shows the curves of total, non-specific and specific binding during incubation at 20 min at room temperature. The values in the plot were corrected by subtracting the non-specific retention of [^{11}C]ML03 in the GF/c filters. This type of filter displayed a very high and inconsistent retention of the labeled compound. Treating them with 0.3% polyethylenimine resulted in a linear retention of [^{11}C]ML03 proportional to the amount added in the assay and in general, in a low number of counts compared to the counts in the samples. As shown in the figure, the maximum specific binding of [^{11}C]ML03 is reached with 80 pmol/tube of [^{11}C]ML03 and corresponds to 67%.

In vivo *results*

In previous work,[22] we carried out *in vivo* biodistribution studies in small animal models, (*i.e.*, tumor-bearing mice). The results of those experiments indicated some specific binding in tumors at 20 min post [^{11}C]ML03 injection. The tumor/blood ratio, however, was below unity. We assumed that the specific binding and the tumor/blood ratio might increase at later time points, therefore we carried out more biodistribution studies at earlier time points and at 30 and 60 min post-tracer injection. In the present experiment we used a larger animal model: tumor-bearing rats. Results are shown in Table I (%id/g and tissue/blood ratios). The highest amount of radioactivity was found in the liver, kidneys and intestine. Values (%id/g) indicated a general decrease of tracer uptake over time in all the organs, excluding the intestine. Compared to the values at 15 min, we obtained the following results at 1 hr post-injection: radioactivity was ½ in tumor, skin and kidneys, ⅓ in blood, ¼ in muscle, heart, lung and spleen, ⅛ in liver and was 3 times higher in the intestine. Normalization of the amount of radioactivity in tissue for the radioactivity in the blood (tissue/

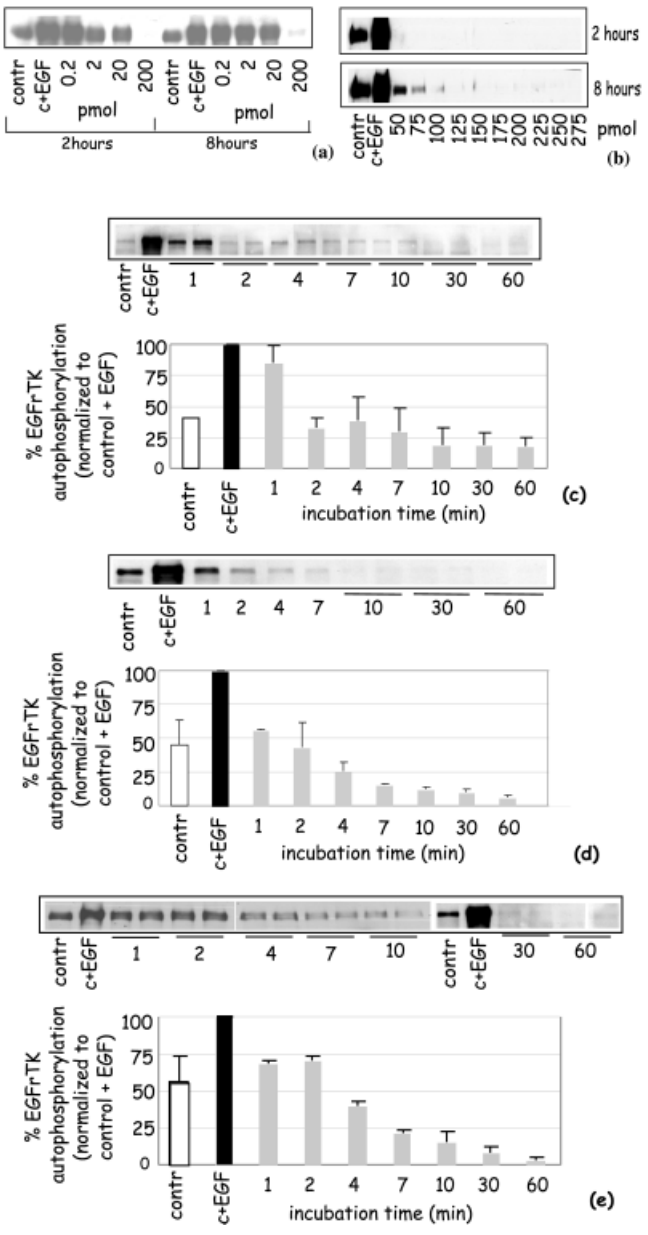

FIGURE 3 – Autophosphorylation of EGFrTK after incubation of A431 cell line with ML03. In all the experiments cells were starved for 18 hours, then incubated with the inhibitor at 37°C or at room temperature and stimulated with EGF either immediately after incubation, or after 2 or 8 hours **(a) (b):** ~2 pmol (a) and ~0.4 pmol (b) of EGFrTK, 2 hours incubation at 37°C, EGF stimulation after 2 and 8 hours. During the 8 hours the medium was changed three times. N = 1 for each amount of ML03. **(c) (d) (e):** Western blots and quantitative analysis of bands (plots). 150 pmol of ML03 and ~1.2 pmol of EGFrTK, incubation at room temperature, stimulation with EGF immediately after incubation (c), after 2 hours (d) and after 8 hours (e). During the 8 hours the medium was not changed. N = 2 for each amount of ML03 (either in the same experiment or in 2 distinct experiments).

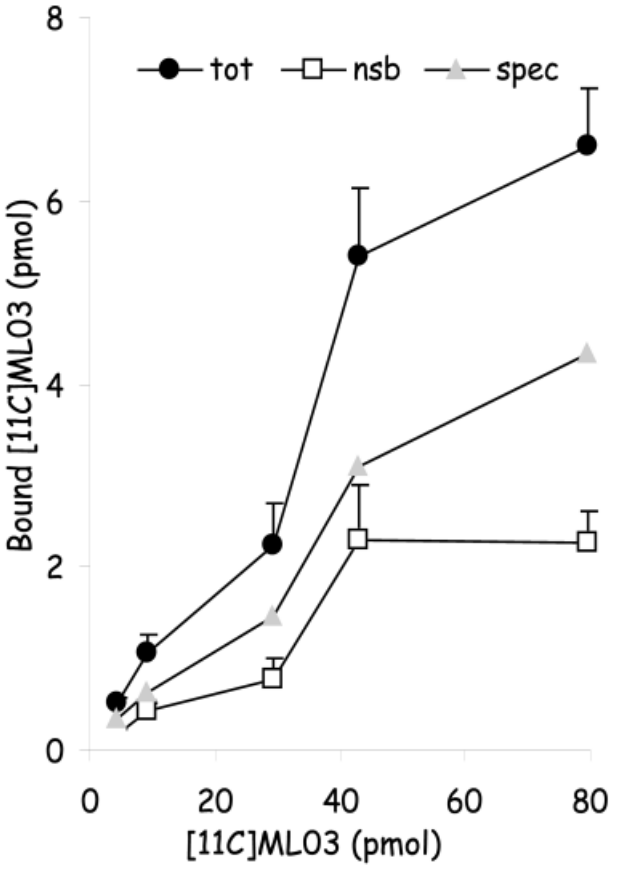

FIGURE 4 – Total (tot), non specific (nsb) and specific (spec) binding of [^{11}C]ML03 in A431 cell line. Values in the plot are counts of sample minus counts of the filter w/o sample (in this case only [^{11}C]ML03 and [^{11}C]ML03 + ML03 were harvested) for total and non specific binding (nsb). The values for the specific binding were obtained by subtraction of the non-specific from the total values. N = 4 (between 5 and 45 pmol) and 8 (for 80 pmol).

blood ratios) also showed a tracer decrease in muscle, heart, lung, liver and spleen. Increase in tissue/blood ratios was observed for tumor, skin, kidneys and intestine. Ratios for tumor/blood, kidney/blood and liver/blood from biodistributions at 15, 30 and 60 min and from partial biodistributions (sacrifice times: 75, 100, 120 min) are shown in Figure 5. Activity in the kidney and liver remained high at all time points. Whereas the liver/blood ratio decreased, the kidney/blood ratio increased. Although the tumor/blood ratio was low, it increased slowly but steadily with time (Fig. 5, see linear regression with $r^2 = 0.7$ and $p = 0.048$), a trend that suggests the possibility of higher tumor/blood ratios at 20–24 hr post-injection, achieving a good target/noise ratio.

Validation of the animal model

We found extreme variability of the tumor morphology. Tumors containing more than 50% of liquid material interfered with our calculation of the % radioactive injected dose per gram, because we could not establish whether this material also contained EGFr. Therefore, we measured the amount of EGFr in intact tumors and correlated it with the tumor mass. Tumors of various masses (from 3–10 g) were extracted from the rats. A random sample of known mass was taken from each frozen tumor and extracted with a proportional volume of extraction buffer (1:5, w/v). Proteins were then measured in the extracts. The amount of extractable proteins was 5.56 ± 0.86 μg per μL of extraction volume, corresponding to 55.58 ± 7.98 mg proteins/g tumor. An equal quantity of protein for each tumor extract was loaded onto polyacrylamide gel for determination of EGFr using Western blot assay. The results are shown in Figure 6. In these plots the means of the EGFr densities are represented by solid lines, whereas dotted lines indicate the 95% interval of confidence. The coefficients of variation are 15.47% and 19.81%. in plots (Fig. 6*a*) and (Fig. 6*b*), respectively. The slight difference between these 2 variances indicates that the variation of EGFr is higher when related to the mass of tumor than when related to the extractable proteins. In both cases, however, we observe that the EGFr density normalized per μg of protein or per g of tumor does not vary with tumor size, suggesting that our tumor animal model is valid and reliable.

Stability and [^{11}C]ML03 metabolism studies

Table II shows the extractable amount of [^{11}C]ML03 from human blood and plasma during 1 hr of incubation and Figure 7*a*, the thin layer radiochromatogram. The extractable amount of radioactivity in blood and plasma was 64.6 % and 83.2%, respectively, at Time Point 0. After 1 hr the extractable radioactivity decreased to 50.2% (blood) and 63.3% (plasma). The TLC radiochromatogram (Fig. 7*a*) showed a single band with RF corresponding to ML03, hence the only extractable radioactivity corresponds to the amount of ML03 still unaltered in blood and plasma. It is likely that the non-extractable fraction of ML03 is the compound itself linked to SH groups of plasma proteins.

Tables III, IV and Figure 7*b* show the results obtained from *in vivo* experiments on [^{11}C]ML03 metabolism in control rats. The extractable fractions of radioactivity from blood (Table III, column B) were 31.6%, 26.1% and 17.1% at 15, 30 and 60 min post-injection, respectively. The extractable fraction seemed to contain 2 radioactive compounds as shown in the TLC (Fig. 7*b*), 1 of them at the same level as the standard [^{11}C]ML03 (band 1) and another above (band 2). The percent ML03 (band 1) in the TLC were 89.8, 83.1 and 74.5% and for the derivative (band 2) 8.4, 16.9, 25.5% at 15, 30 and 60 min, respectively (Table III, column C). Only 0.054% id/g of extractable ML03 in blood is not metabolized and available for further binding at 15 min (Table III, column D); the extractable metabolite is 0.006% id/g at this time point. If we consider the radioactivity in blood as 100% (without normalization for the injected dose), the amounts of intact and available ML03 are 28.3%, 20.9% and 11.7% at 15, 30 and 60 min, respectively (Table III, column E), indicating that the half-life of our compound in blood is of the order of a few minutes. Conversely, the only detectable and extractable metabolite increases up to 3.95% during 1 hr (Table III, column E).

In another set of studies we measured the intact ML03 in liver (and again in blood) at 15 and 30 min post-injection. Table IV and Figure 7*b* show the results. The total amounts of radioactivity extractable from the liver were 9.3% (15 min) and 13.3% (30 min). From this fraction, 2 radioactive bands were found on the TLC as observed in blood (Fig. 7*b*). The amounts of extractable non-metabolized ML03 (band 1) were 0.151 and 0.047 %id per g of liver at 15 and 30 min, respectively, whereas amounts of unknown extractable metabolite (band 2) were 0.016 and 0.020 %id/g liver, respectively. Considering the radioactivity in the liver as 100%, at 15 and 30 min, 8–9% corresponded to ML03, whereas 0.9–3.9% corresponded to a metabolite; at the same time points, 91% and 87% respectively, was unextractable radioactivity. These values confirm that our compound is metabolized rapidly and already cleared from the body in the first 15–30 min with production of other radioactive compounds.

PET studies

Figure 9 illustrates coronal sections (frames from 15–60 min) of A431 tumor-bearing rats injected with [^{18}F]FDG (Fig. 9*a*) or [^{11}C]ML03 (Fig. 9*b*). In all images the contour of the attenuation scan has been superimposed on the emission images to locate tumor position and accumulation of radioactivity. Scans with both tracers were carried out, in different days, on Rat 1, to compare the body distribution. As shown by the red cursor, in Rat 1 the tumor was positioned in the leg. After injection of [^{18}F]FDG the tumor

TABLE I – BIODISTRIBUTION OF [^{11}C]ML03 IN TUMOR-BEARING RATS (*rnu/rnu*)

	15 min	30 min	1 hr
% id/g			
Blood	0.166 ± 0.063	0.123 ± 0.029	0.051 ± 0.012
Tumor	0.090 ± 0.039	0.089 ± 0.016	0.050 ± 0.012
Skin	0.071 ± 0.031	0.078 ± 0.024	0.038 ± 0.013
Muscle	0.087 ± 0.040	0.057 ± 0.020	0.022 ± 0.006
Heart	0.174 ± 0.059	0.113 ± 0.030	0.043 ± 0.013
Lung	0.251 ± 0.087	0.169 ± 0.048	0.065 ± 0.016
Liver	1.844 ± 0.682	0.902 ± 0.347	0.239 ± 0.091
Kidneys	0.729 ± 0.336	0.711 ± 0.177	0.322 ± 0.096
Spleen	0.156 ± 0.050	0.100 ± 0.020	0.044 ± 0.010
Intestine	1.146 ± 0.707	3.402 ± 0.612	3.744 ± 0.599
Tissue/blood			
Tumor	0.537 ± 0.035	0.750 ± 0.222	0.969 ± 0.050
Skin	0.433 ± 0.146	0.632 ± 0.069	0.738 ± 0.210
Muscle	0.510 ± 0.094	0.456 ± 0.057	0.424 ± 0.039
Heart	1.067 ± 0.072	0.911 ± 0.060	0.828 ± 0.050
Lung	1.530 ± 0.074	1.371 ± 0.126	1.269 ± 0.055
Liver	11.202 ± 1.702	7.189 ± 1.112	4.643 ± 1.126
Kidneys	4.282 ± 0.412	5.777 ± 0.480	6.235 ± 0.384
Spleen	0.958 ± 0.089	0.826 ± 0.135	0.867 ± 0.053
Intestine	5.734 ± 2.319	29.205 ± 10.518	75.256 ± 17.459

[1]Values (%id/g and the corresponding tissue/blood ratios) are averages ± SD (15 min, $n = 4$; 30 min, $n = 5$; 1 hr, $n = 3$).

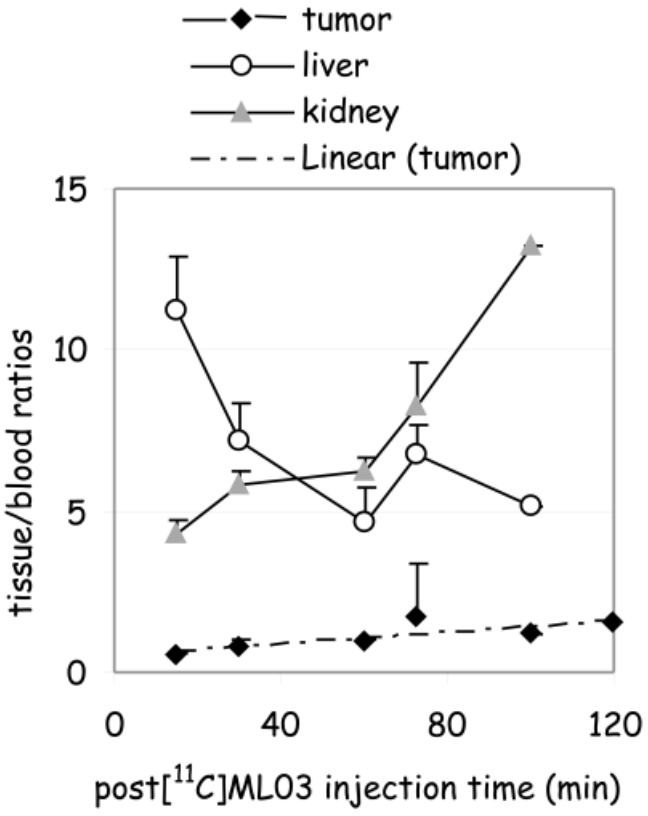

FIGURE 5 – Tumor, liver, kidneys/blood ratios vs post [^{11}C]ML03 injection time in tumor-bearing rat biodistributions. N = 5 (30 min), 4 (15, 60 min), 2 (73 min), 1 (100 min) and 1 only for tumor (120 min). For tumor, the linear regression is shown ($r^2 = 0.7$, P = 0.048).

was detectable, whereas when the same rat was injected with [^{11}C]ML03 (5 days later) radioactivity accumulation was mainly in the intestine. In this rat the tumor was not visualized and the partial biodistribution carried out after the scan showed tumor/blood, tumor/skin, tumor/muscle and tumor/heart ratios of 2.86, 3.53, 4.61 and 2.69, respectively. These results confirm the limited accumulation of the tracer in the tumor observed in the *ex vivo* biodistribution experiments, and the intestine as main organ of accumulation of radioactivity during the hour post-tracer injection.

DISCUSSION

Radiochemistry

Labeling ML03 with fluorine-18 was considered initially due to its longer half-life of 110 minutes. Introducing fluorine-18 into ML03, however, would involve 5 radiosynthesis steps. Labeling would be the first step. Both the long synthesis time and the difficulties associated with automatic procedure did not favor labeling with fluorine-18. Labeling with carbon-11, on the other hand, enabled us to carry out the introduction of the radioisotope into the molecule as the last step of the synthesis and permitted easy automation, using 1-[C-11]acryloyl chloride as the labeling synthon. Radiosynthesis of [C-11]α,β-unsaturated acyl derivatives is already known, although their use as labeling synthons is quite limited. The [C-11]acryloyl chloride synthon was used to label ML03, with 6-amino-4-(3-4dichloro-6-fluoro)-quinazoline as precursor. ML03 was produced in 13% recovered radiochemical yield (EOB) in 45 min synthesis time (including purification). The radiosynthesis was reliable and reproducible ($n > 35$) yielding 8–15 mCi of ML03, sufficient for future human use. HPLC analysis of the product solution showed high radiochemical (>99%) and chemical purities (final product containing 0.5–3 ppm of remaining precursor). The specific radioactivity achieved in the radiosynthesis was up to 1.8 Ci/μmol (EOB).

In vitro *studies*

Results from the *in vitro* experiments with unlabeled and labeled ML03 demonstrated that ML03 possesses high affinity for EGFr and irreversibly inhibits the autophosphorylation of the receptor (Fig. 3). The experiments described with intact A431 cells show that the effect of ML03 is very rapid, reaching ~80% 10 min after exposure to the compound. In Figure 3*b* we observe a restored autophosphorylation activity 8 hr post-incubation with 50 and 75 pmol of ML03. This partially restored TK activity is due to the wash-out carried out during the 8 hr post-injection. During this time, the medium was changed 3 times with fresh ML03/FCS-free medium. The removal of the medium washed away the ML03 that was still unbound after 2 hr of incubation and had diffused through the membrane to the medium. It is likely that after the wash out the inhibitor remaining inside the cell is not enough to bind more

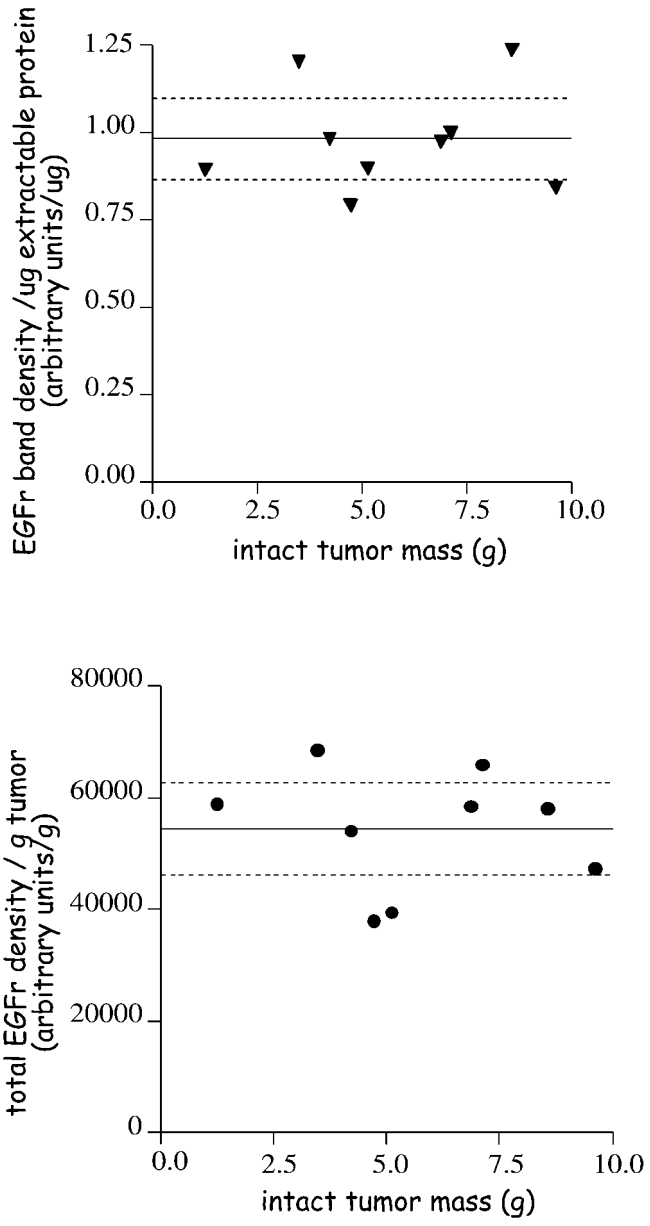

FIGURE 6 – Validation of the tumor-bearing model. Tumors were extracted and part of the extraction was loaded in acrylamide gel for the Western blot assay (n = 9). The y values in (a) and (b) are the experimental EGFr densities of the gel bands versus the total intact tumor mass (a), and the total EGFr densities (= experimental densities values/μL loaded on gel × the total tumor extraction volume) versus the total intact tumor mass.

EGFr or inhibit the newly synthesized EGFr. Because the wash out was not carried out in (Fig. 3*e*), we do not observe any EGFr recovery in the autophosphorylation activity. These data suggest that ML03 is stable for 8 hr. In this regard, comparing Figure 3*c* and Figure 3*e*, the percent of inhibition in the 8 hr after the 60-min ML03 incubation is estimated to be approximately an additional 15%, because the ML03 that diffused into the cell during the incubation period was never removed by the wash out procedure. As a result, there was an increased receptor inhibition in Figure 3*e*, (97.5% inhibition) compared to the inhibition in Figure 3*c* (82.5%).

Studies with labeled ML03 also demonstrate that ML03 shows high affinity for the EGFr. We recovered up to 67% of the specific

TABLE II – PERCENT OF EXTRACTABLE [^{11}C]ML03 FROM HUMAN BLOOD AND PLASMA[1]

Minutes	Blood	Plasma
0	64.6 ± 11.2	83.2 ± 6.9
10	68.5 ± 6.3	80.0 ± 8.9
20	57.3 ± 8.0	68.7 ± 10.8
30	53.5 ± 8.8	68.4 ± 11.8
40	55.0 ± 2.5	69.2 ± 8.7
50	44.4 ± 13.3	68.0 ± 2.8
60	50.2 ± 5.4	63.3 ± 9.6

[1]The tracer was incubated at the indicated times at 37°C (except for 0 min) and extracted with ether. Pre- and post-extraction fractions were then counted. Values are the average ± SD (n = 3 for blood at 0, 20, 40 and 60 min, and plasma at 20, 40 and 60 min of incubation; n = 2 for blood 10, 30 and 50 min, and plasma 0, 10, 30 and 50 min of incubation).

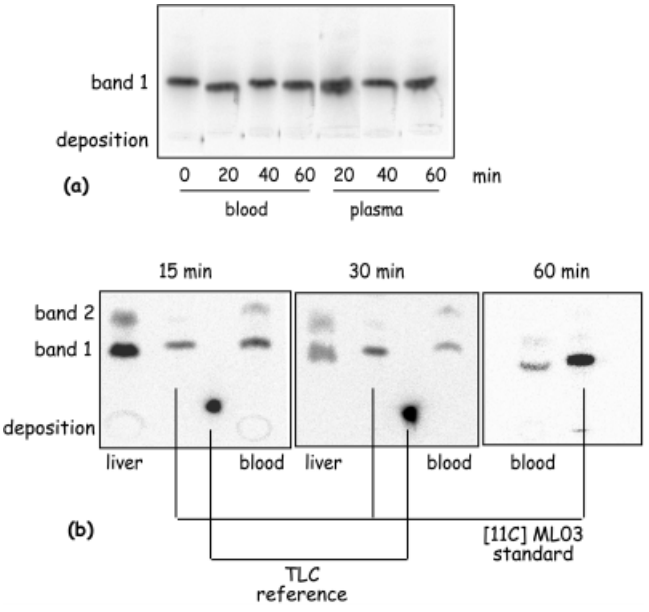

FIGURE 7 – Stability of [^{11}C]ML03 in human blood (a) and metabolism in blood and liver from control rats (b). (a) TLC of extracted radioactive fractions from human blood and plasma after incubation with [^{11}C]ML03 at 37°C (time points 0, 20, 40, 60 min for blood and 20, 40, 60 for plasma). (b) TLC of extracted fractions from blood and liver of control rats after [^{11}C]ML03 injection (time points 15, 30, 60 minutes for blood and 15, 30 minutes for liver). The samples from liver and blood at 15 and 30 minutes are from the same animal.

binding. At this specific binding, the amount of inhibitor bound to EGFr is ~4 pmol. This value is in agreement with the calculated amount of EGFr used for the assay, indirectly indicating the selectivity of ML03 to EGFr.

In vivo *studies*

In the validation of the animal model experiments, random samples from different tumors with variable mass were extracted. The total EGFr density per g of tumor was found to be constant in all the samples. Distribution and density of EGFr was also homogeneous within the tumor, despite morphological differences, and independent of the tumor size.

By means of our tumor model we checked the biodistribution of ML03. ML03 does not accumulate specifically in the target tumor, however the trend of the tumor/blood ratios (Fig. 5) suggests that this ratio might improve at longer times. Considering that metabromo derivatives of 6-acrylamido-4-anilinoquinazolines were found to be potent and selective in cell studies,[20,23] labeling ML03

TABLE III – METABOLISM OF [^{11}C] ML03 IN BLOOD FROM CONTROL RATS (*rnu/+*)[1]

Minutes	*n*	A	B	C	D	E
15		0.203 ± 0.068	0.316 ± 0.112			
30		0.147 ± 0.044	0.261 ± 0.109			
60		0.107 ± 0.040	0.171 ± 0.040			
Band 1						
15	6			0.898 ± 0.041	0.054 ± 0.018	28.304 ± 12.756
30	5			0.831 ± 0.065	0.025 ± 0.011	20.934 ± 11.965
60	3			0.745 ± 0.056	0.011 ± 0.003	11.692 ± 3.819
Band 2						
15	5			0.084 ± 0.029	0.006 ± 0.003	2.734 ± 1.418
30	5			0.169 ± 0.065	0.005 ± 0.001	3.788 ± 1.377
60	3			0.255 ± 0.056	0.004 ± 0.000	3.952 ± 1.289

[1]Values are from blood samples withdrawn from the same animal at 15, 30 and 60 min post [^{11}C] ML03 injection. Each sample was extracted with ether, spotted onto TLC, and exposed to phosphoimager plates after the run. The values are averages ± SD. Band 1 and band 2, radioactive bands in the TLC; *n,* number of animals; A, %id/g of radioactivity in blood; B, radioactivity fraction extracted from blood [1-(post extraction counts/pre extraction counts)]; C, radioactivity fractions on TLC after the run and detected by phosphor imaging plate (1 as total radioactivity recovered in the TLC); D, extractable normalized by the %id/g (A × B × C); E, B × C (in %).

TABLE IV – METABOLISM OF [^{11}C] ML03 IN BLOOD AND LIVER FROM CONTROL RATS (*rnu/+*)[1]

Tissue	Minutes	*n*	A	B	C	D	E
Blood	15	2	0.215 ± 0.036	0.314 ± 0.045			
	30	3	0.075 ± 0.006	0.284 ± 0.019			
Liver	15	2	1.842 ± 0.240	0.093 ± 0.031			
	30	3	0.511 ± 0.051	0.133 ± 0.077			
Band 1							
Blood	15	2			0.827 ± 0.019	0.055 ± 0.000	25.988 ± 4.337
	30	3			0.620 ± 0.107	0.013 ± 0.003	17.544 ± 2.342
Liver	15	2			0.899 ± 0.025	0.151 ± 0.036	8.399 ± 3.039
	30	3			0.705 ± 0.010	0.047 ± 0.027	9.339 ± 5.326
Band 2							
Blood	15	2			0.173 ± 0.019	0.012 ± 0.002	5.376 ± 0.152
	30	3			0.380 ± 0.107	0.008 ± 0.002	10.877 ± 3.474
Liver	15	2			0.101 ± 0.025	0.016 ± 0.001	0.901 ± 0.085
	30	3			0.295 ± 0.010	0.020 ± 0.012	3.936 ± 2.360

[1]Blood and liver results at 15 and 30 min post [^{11}C] ML03 injection are from the same animal for each time. Each sample was extracted with ether, spotted onto TLC, and exposed to phosphoimager plates after the run. The values are averages ± SD. Band 1 and band 2, radioactive bands in the TLC; *n,* number of animals; A, %id/g of radioactivity in blood or liver; B, radioactivity fraction extracted from blood or liver [1-(post extraction counts/pre extraction counts)]; C, radioactivity fractions on TLC after the run and detected by phosphor imaging plate (1 as total radioactivity recovered in the TLC); D, extractable normalized by the %id/g (A × B × C); E, B × C (in %).

with a longer half-life positron emitter radioisotope such as ^{76}Br ($t_{1/2}$ = 16.2 hr), would probably be more suitable for investigating the potential improvement of target/noise ratio with the time. The fast decrease of liver/blood ratios and the increase of kidney/blood and intestine/blood ratios suggest that the liver metabolizes ML03 and then a portion of it goes to the kidney, whereas another portion is secreted into the intestinal tract (hepatobiliary clearance). In the latter case, some metabolites are excreted in the feces although some of them can be reabsorbed into the blood and ultimately excreted with the urine. The rapid increase of the intestine/blood ratio implies that the secretion in the intestinal tract is the main excretion pathway. The radioactivity found in the excretory organs is not due to instability of ML03. As shown in blood and plasma (Fig. 7*a*), ML03 is stable within 1 hr of incubation at 37°C. The high percent of unextractable radioactivity is most probably due to the high chemical reactivity of the acryloyl group. The hepatic involvement in the decomposition of our compound is clear from the studies in control animals. At 15 min post-injection, 68% of ML03 is not extractable from the blood and therefore no longer available for targeting the tumor, and part of the extractable fraction is already converted to other molecules. One of the hypothesized derivatives of ML03 that could correspond to this extractable metabolite (band 2 in Fig. 7*b*) is acrylquinazolone (Fig. 8*a*). The formation of the diclorofluoroanilinoquinazoline (Fig. 8*b*) can be excluded, because we did not detect radioactive acryloyl band in any of the TLC.

Among the biodistribution experiments, a preliminary *in vivo* blocking study at 30 min (not described in our article) was carried out without achieving any specific binding, in contrast to previous studies with mice[22] where we observed specific binding in the tumor. This could be explained by high non-specific binding, degradation and low bioavailability of ML03 and the difficulties to block high capacity systems (B_{max} in rat is proportionally higher than in mouse). Because the tracer accumulation in the tumor was low compared to other organs, we concluded that additional blocking experiments in rats with [^{11}C]ML03 were unnecessary.

PET images

As seen in Figure 9*a*,*b* the tumor is not visualized in Rat 1 after [^{11}C]ML03 injection, although the major accumulation of radioactivity is in the gut, confirming the results obtained in the biodistribution studies (Table I). The resulting conclusion is that ML03 is degraded into several metabolites, one of them extractable, but in a very low amount (Fig. 7b), whereas the major part of ML03 (non-extractable) is converted into hydrophilic molecules with the intestine as main excretion pathway. Figure 9*c* shows a PET image of A431 tumor-bearing mice injected with [^{18}F]FDG (Fig. 9*c*, top) and with a reversible inhibitor labeled previously[15] (Fig. 9*c*, bottom) for comparison with [^{11}C]ML03. Although we did not use a specialized high resolution animal PET scanner and despite the smaller size of the animal model, we could visualize the tumor on the leg of the mice with [^{18}F]FDG and with our reversible inhibitor. In the case of the reversible inhibitor, although the tumor/blood ratio was below unity, we could at least define a weak signal in the time window of highest uptake in the tumor. Considering also that with both the reversible and irreversible inhibi-

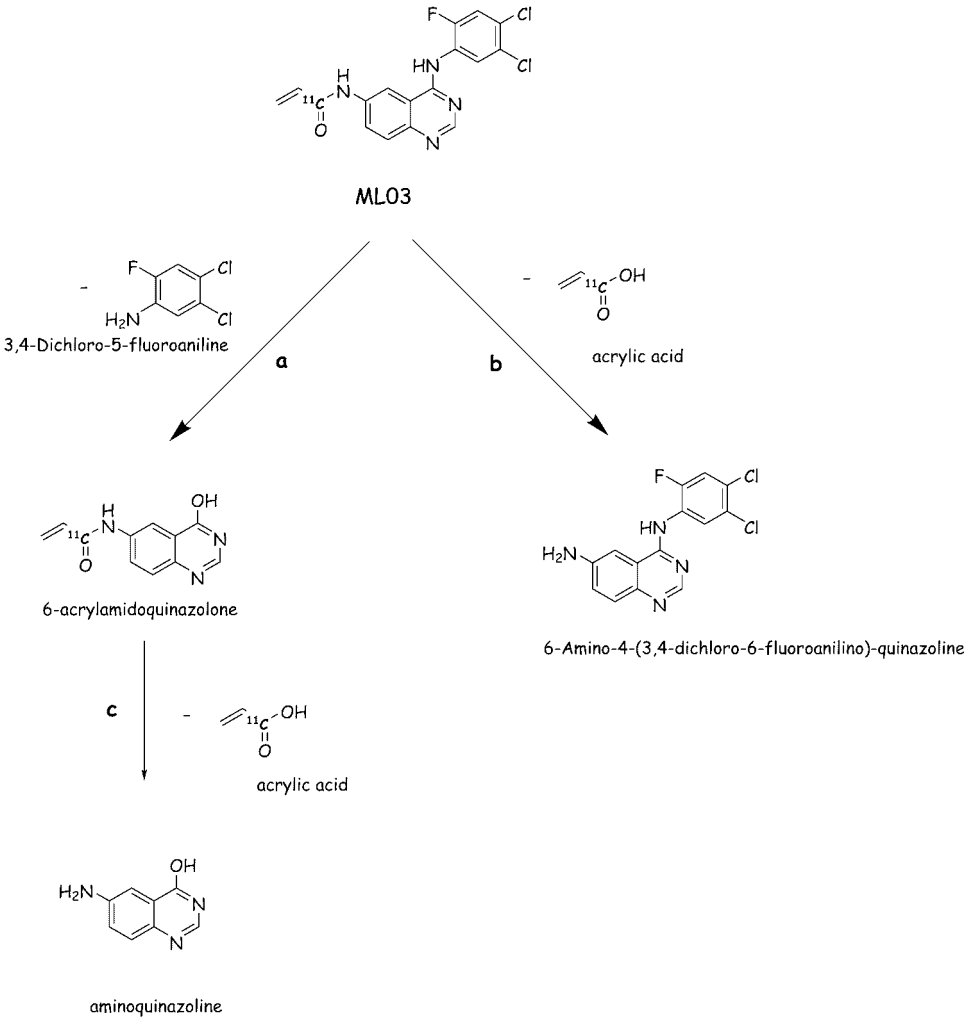

FIGURE 8 – Hypothetical pathways of degradation of ML03.

tors, the rate of degradation is very similar, we expected to have a weak signal from the PET studies with [^{11}C]ML03 as well. In conclusion, although the irreversible inhibitor eliminates the problem of displacement and competition with ATP seen with reversible inhibitors, degradation and bioavailability of ML03 remain consistent impediments preventing visualization of the tumor by PET.

ML03 bioavailability

The fast clearance of ML03 raised questions about its bioavailability. ML03 and similar compounds are highly hydrophobic and non-soluble in aqueous solutions. Thinking about the next generation of PET biomarkers, one should consider the possibility of modifying synthesis and radiolabeling to generate compounds that are more hydrophilic and therefore have increased bioavailability. One way to predict these properties is to calculate the predictable *LogP* and $LogD_{pH7}$. We calculated *LogP* and $LogD_{pH7}$ values (ACDLabs Chem Sketch software) as bioavailability index for ML03 and for many other compounds that are described in the literature as molecules with high affinity for EGFr-TK and have been selected for clinical trials. *LogP* and $LogD_{pH7}$ for ML03 were 3.87 *P* 1.15 and 3.9 *P* 1.0, respectively. For molecules such as ZD-1839, OSI-774, CI-1033 and a cyanoquinoline described by Renhowe[24] as compounds in clinical trial, *LogP* and $LogD_{pH7}$ were 4.05 and 3.6 (ZD-1839), 2.46 and 2.4 (OSI-774), 3.59 and 3.1 (CI-1033) and 6.06 and 4.9 (cyanoquinoline), respectively. Although these values are theoretical, the wide *LogP* and $LogD_{pH7}$ range in compounds that are in clinical trials indicates that this parameter is not sufficient to predict which molecule could be useful for therapeutic use or as a PET biomarker for diagnostics.

CONCLUSION

We synthesized and radiolabeled with ^{11}C the acrylamide quinazoline derivative ML03 as a candidate for PET imaging of cancers overexpressing EGFr-TK. This compound showed high potency for the receptor in A431 cells and its binding effect was irreversible and fast, reaching 80% inhibition after 10 min. ML03 showed specific binding in A431 cells (67%). Compared to the *in vitro* results with our previous reversible inhibitor,[15] ML03 showed higher potency. A tumor model that proved to be valid and reliable was developed to study and evaluate PET biomarkers targeting EGFr-TK. The *in vivo* studies in tumor-bearing rats did not indicate high accumulation of [^{11}C]ML03 in the tumor. The tumor/blood ratio increased with time, however, suggesting that a longer half-life isotope might be more suitable for labeling ML03. In the experiments on metabolism we observed fast decomposition and clearance of the compound. The *in vivo* results were confirmed by PET studies where the images clearly showed a very high accumulation in the intestine, the most likely excretory organ for ML03. These results suggest the low bioavailability of ML03 as the main parameter preventing greater accumulation of ML03 in the target. This major problem makes ML03 less

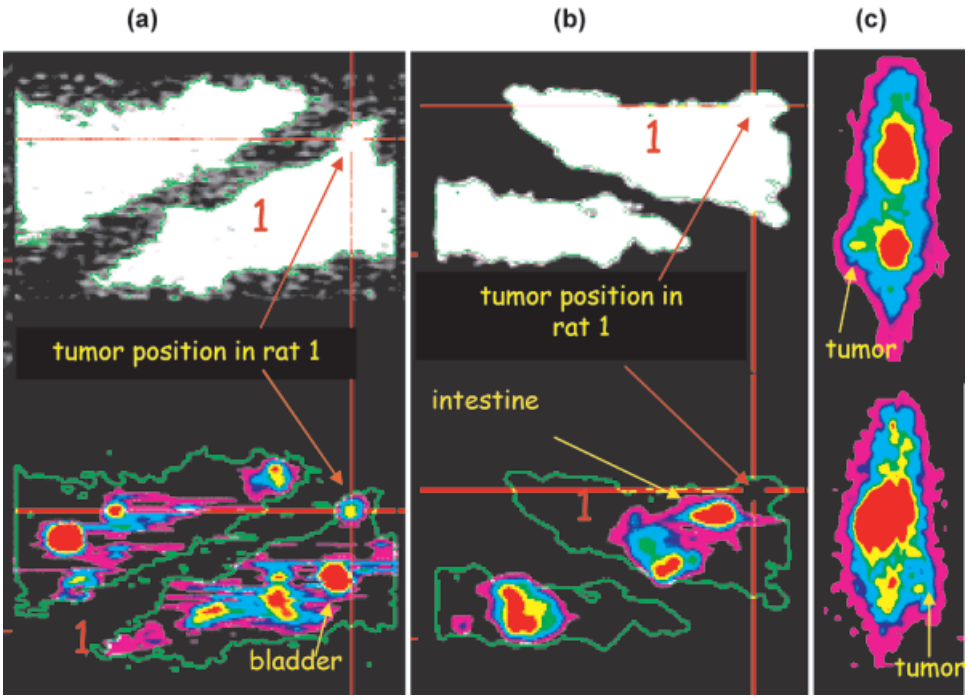

FIGURE 9 – PET images of A431 tumor-bearing rats injected with [^{18}F]FDG (a), or [^{11}C]ML03 (b), and PET images of A431 tumor-bearing mice injected with [^{18}F]FDG (c, top) and a previously reported reversible inhibitor (Bonasera et al. 2001) (c, bottom). The shown coronal sections are the sum of frames between 15 and 60 minutes for (a) and (b), 45–50 minutes (c, top), and 8–12 minutes (c, bottom). Red cursors indicate the tumor position in the attenuation scan (a and b, top), and in the PET image (a and b, bottom).

suitable as a PET tracer than our previous reversible compound. Micro-PET studies with different tumor animal models and different specific activity should also be done to clarify doubts on the correlation between B_{max} in tumor, size of the animal model and injected mass. Moreover, additional irreversible tyrosine kinase inhibitors with lower metabolic rate and higher bioavailability should be synthesized and labeled with ^{76}Br and ^{124}I to measure the tumor accumulation of this type of compound at later time points.

ACKNOWLEDGEMENTS

Support was provided by the USA-Israel Bi-national Science Foundation (BSF 98000082, to EM and AL).

REFERENCES

1. Arteaga CL. The epidermal growth factor receptor: from mutant oncogene in nonhuman cancers to therapeutic target in human neoplasia. J Clin Oncol 2001;19:32–40.
2. Voldborg BR, Damstrup L, Spang-Thomsen M, Poulsen HS. Epidermal growth factor receptor (EGFR) and EGFR mutations, function and possible role in clinical trials. Ann Oncol 1997;8:1197–206.
3. Raymond E, Faivre S, Armand JP. Epidermal growth factor receptor tyrosine kinase as a target for anticancer therapy. Drugs 2000;60:15–23; discussion 41–2.
4. Yaish P, Gazit A, Gilon C, Levitzki A. Blocking of EGF-dependent cell proliferation by EGF receptor kinase inhibitors. Science 1988; 242:933–5.
5. Gazit A, Osherov N, Gilon C, Levitzki A. Tyrphostins. 6. Dimeric benzylidenemalononitrile tyrophostins: potent inhibitors of EGF receptor tyrosine kinase *in vitro*. J Med Chem 1996;39:4905–11.
6. Gazit A, Chen J, App H, McMahon G, Hirth P, Chen I, Levitzki A. Tyrphostins IV—highly potent inhibitors of EGF receptor kinase. Structure-activity relationship study of 4-anilidoquinazolines. Bioorg Med Chem 1996;4:1203–7.
7. Ben-Bassat H, Vardi DV, Gazit A, Klaus SN, Chaouat M, Hartzstark Z, Levitzki A. Tyrphostins suppress the growth of psoriatic keratinocytes. Exp Dermatol 1995;4:82–8.
8. Levitzki A, Gazit A. Tyrosine kinase inhibition: an approach to drug development. Science 1995;267:1782–8.
9. Fry DW, Kraker AJ, McMichael A, Ambroso LA, Nelson JM, Leopold WR, Connors RW, Bridges AJ. A specific inhibitor of the epidermal growth factor receptor tyrosine kinase. Science 1994;265: 1093–5.
10. Fry DW, McMichael A, Singh J, Dobrusin EM, McNamara DJ. Design of a potent peptide inhibitor of the epidermal growth factor receptor tyrosine kinase utilizing sequences based on the natural phosphorylation sites of phospholipase C-gamma 1. Peptides 1994; 15:951–7.
11. Kunkel MW, Hook KE, Howard CT, Przybranowski S, Roberts BJ, Elliott WL, Leopold WR. Inhibition of the epidermal growth factor receptor tyrosine kinase by PD153035 in human A431 tumors in athymic nude mice. Invest New Drugs 1996;13:295–302.
12. Fredriksson A, Johnstrom P, Thorell JO, von Heijne G, Hassan M, Eksborg S, Kogner P, Borgstrom P, Ingvar M, Stone-Elander S. *In vivo* evaluation of the biodistribution of ^{11}C-labeled PD153035 in rats without and with neuroblastoma implants. Life Sci 1999;65:165–74.
13. Mulholland GK, Winkle W, Mock BH, Sledge G. Radioiodinated epidermal growth factor receptor ligands as tumor probes. Dramatic potentiation of binding to MDA-468 cancer cells in presence of EGF. J Nucl Med 1995;36(Suppl):71P.
14. Mulholland GK, Zheng Q-H, Winkle WL, Carlson KA. Synthesis and biodistribution of new C-11 and F-18 labeled epidermal growth factor receptor ligands. J Nucl Med 1997;38(Suppl):141P.
15. Bonasera TA, Ortu G, Rozen Y, Krais R, Freedman NM, Chisin R, Gazit A, Levitzki, A Mishani E. Potential (18)F-labeled biomarkers for epidermal growth factor receptor tyrosine kinase. Nucl Med Biol 2001;28:359–74.
16. Vincent PW, Bridges AJ, Dykes DJ, Fry DW, Leopold WR, Patmore SJ, Roberts BJ, Rose S, Sherwood V, Zhou H, Elliott WL. Anticancer efficacy of the irreversible EGFr tyrosine kinase inhibitor PD 0169414 against human tumor xenografts. Cancer Chemother Pharmacol 2000; 45:231–8.
17. Smaill JB, Palmer BD, Rewcastle GW, Denny WA, McNamara DJ, Dobrusin EM, Bridges AJ, Zhou H, Showalter HD, Winters RT, Leopold WR, Fry DW, et al. Tyrosine kinase inhibitors. 15. 4-(Phenylamino)quinazoline and 4-(phenylamino)pyrido[d]pyrimidine acrylamides as irreversible inhibitors of the ATP binding site of the epidermal growth factor receptor. J Med Chem 1999; 42:1803–15.
18. Smaill JB, Rewcastle GW, Loo JA, Greis KD, Chan OH, Reyner EL, Lipka E, Showalter HD, Vincent PW, Elliott WL, Denny WA. Tyrosine kinase inhibitors. 17. Irreversible inhibitors of the epidermal growth factor receptor: 4-(Phenylamino)quinazoline- and 4-(Phenylamino)pyrido. J Med Chem 2000;43:1380–97.
19. Smaill JB, Rewcastle GW, Loo JA, Greis KD, Chan OH, Reyner EL, Lipka E, Showalter HD, Vincent PW, Elliott WL, Denny WA. Ty-

rosine kinase inhibitors. 17. Irreversible inhibitors of the epidermal growth factor receptor: 4-(Phenylamino)quinazoline- and 4-(Phenylamino)pyrido. J Med Chem 2000;43:3199.
20. Tsou HR, Mamuya N, Johnson BD, Reich MF, Gruber BC, Ye F, Nilakantan R, Shen R, Discafani C, DeBlanc R, Davis R, Koehn FE, et al. 6-Substituted-4-(3-bromophenylamino)quinazolines as putative irreversible inhibitors of the epidermal growth factor receptor (EGFR) and human epidermal growth factor receptor (HER-2) tyrosine kinases with enhanced antitumor activity. J Med Chem 2001;44:2719–34.
21. Mishani E, Ben-David I, Rozen Y, Ortu G, Leviztki A. Carbon-11 labeled irreversible inhibitor for mapping epidermal growth factor receptor tyrosine kinase (EGFr-TK). J Labeled Comp Radiopharm 2001;44(Suppl):S99.
22. Ortu G, Ben-David I, Rozen Y, Levitzki A, Mishani E. Biological evaluation of a novel (11-C)labeled irreversible EGFRTK inhibitor. Q J Nucl Med 2001;45:S7.
23. Fry DW, Bridges AJ, Denny WA, Doherty A, Greis KD, Hicks JL, Hook KE, Keller PR, Leopold WR, Loo JA, McNamara DJ, Nelson JM, et al. Specific, irreversible inactivation of the epidermal growth factor receptor and erbB2, by a new class of tyrosine kinase inhibitor. Proc Natl Acad Sci USA 1998;95:12022–7.
24. Renhowe PA. Growth factor receptor kinases in cancer. Annu Rep Med Chem 2001;36:109–18.